Defense Technical Information Center Compilation Part Notice

ADP012315

TITLE: Exploring the Limits of Fast Phase Change Materials

DISTRIBUTION: Approved for public release, distribution unlimited

This paper is part of the following report:

TITLE: Applications of Ferromagnetic and Optical Materials, Storage and Magnetoelectronics: Symposia Held in San Francisco, California, U.S.A. on April 16-20, 2001

To order the complete compilation report, use: ADA402512

The following component part numbers comprise the compilation report:
ADP012260 thru ADP012329

Mat. Res. Soc. Symp. Proc. Vol. 674 © 2001 Materials Research Society

Exploring the limits of fast phase change materials

Han-Willem Wöltgens, Ralf Detemple, Inés Friedrich, Walter K. Njoroge, Ingo Thomas, Volker Weidenhof, Stefan Ziegler, Matthias Wuttig
I. Physikalisches Institut der RWTH-Aachen, D-52056 Aachen, Germany

Abstract

In the last decade a number of chalcogenide alloys, including ternary alloys of GeSbTe and quaternary alloys of InAgSbTe, have been identified which enable fast phase change recording. In the quest for materials with improved phase change kinetics we present two different approaches. By comparing alloys with well-defined stoichiometries the mechanisms which govern the transformation kinetics are determined. Optical and electrical measurements determine the activation energy for crystallization to 2.24 ± 0.11 eV for $Ge_2Sb_2Te_5$ and to 3.71 ± 0.07 eV for $Ge_4Sb_1Te_5$, respectively. It is shown that for GeSbTe-alloys with different composition the activation energy increases linearly with increasing Ge content. Power-time-reflectivity change diagrams recorded with a static tester reveal that $Ge_2Sb_2Te_5$, in agreement with previous data, recrystallizes by the growth of sub critical nuclei, while $Ge_4Sb_1Te_5$ grows from the crystalline rim surrounding the bit.

To speed up the search for faster materials we employ concepts of combinatorial material synthesis by producing films with a stoichiometry gradient. Then laterally resolved secondary neutral mass spectroscopy (SNMS) combined with the static tester are used to identify the composition with superior properties for phase change applications.

INTRODUCTION

Materials at the pseudo-binary line $(GeTe)_x(Sb_2Te_3)_{1-x}$ are known to have good properties for fast phase change applications [1,2]. Nevertheless we need to characterize and understand the transformation kinetics of these materials if we want to develop a microscopic understanding of phase change dynamics. Hence, we have investigated the phase transformation on a microscopic and macroscopic scale for two compounds along the pseudo-binary line.

From the understanding of the transformation kinetics for these compounds we try to obtain insight into the behaviour expected for an arbitrary compound like $A_\alpha B_\beta C_\gamma Te$. Then combinatorial concepts in conjunction with efficient strategies to measure transformation kinetics are applied to further improve our understanding of the kinetics and the properties of phase change materials.

EXPERIMENTAL DETAILS

The GeSbTe-compounds used for microscopic and macroscopic studies were deposited on glass or silicon substrates at room temperature by dc magnetron sputtering [3]. A static tester as described in [4] is used to measure the reflectance change upon short laser pulse irradiation. The sheet resistance was measured with a four-point probe setup following the procedure proposed by van der Pauw [5]. Further experimental details are already described elsewhere [6]. x-ray refractometry (XRR) measurements were performed to determine the thickness, roughness and the density while x-ray diffractometry (XRD) measurements were used to determine the film structure at room temperature.

The Sb_xTe_{1-x} sample was evaporated onto glass in an molecular beam epitaxy (MBE) system designed for combinatorial synthesis. The background pressure of the evaporation system is 3 ×

10^{-10} mbar. Up to five evaporation sources can be assembled into the system to prepare multi element thin films with any desired stoichiometry. Up to four evaporators can be aligned under 45 degrees with respect to the sample normal. Basic emission laws show that the film thickness distribution then will be inhomogeneous [7]. A fifth source can be inserted perpendicular to the sample. Superposing the thickness distributions of the different elements will lead to lateral stoichiometry gradients. In this situation, the exact composition of the samples can then be controlled by adjusting the evaporation rate of the different sources. The stoichiometry gradient is then determined by in situ secondary neutral mass spectrometry (SNMS), so that we know the exact composition of the sample for different positions. Finally, a static tester is used to characterize the behaviour of these samples.

RESULTS AND DISCUSSION

In the following we will first discuss macroscopic measurements to characterize the crystallization behaviour. Subsequently, microscopic measurements are employed to determine the crystallization mechanism. Finally first results from samples prepared by combinatorial methods are presented.

Temperature dependent measurements of the electrical resistance are very sensitive to the phase transition since the resistance is changing over several orders of magnitude at the critical temperature T_C. This enables a precise determination of the transition temperature. From the change in T_C as a function of heating rate the effective activation energy for exothermal crystallization for the specific phase transition can be determined using Kissinger plots [8]. Figure 1 shows the temperature dependence of the sheet resistance (R_S) of 80 nm thin $Ge_2Sb_2Te_5$ and $Ge_4Sb_1Te_5$ films.

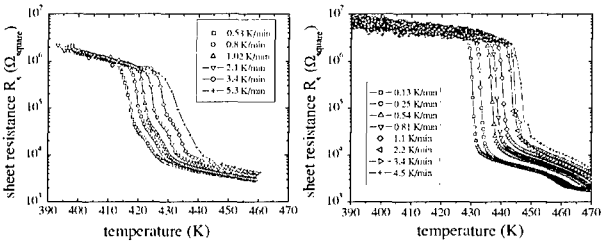

Figure 1. Temperature dependence of the sheet resistance R_S of 80 nm $Ge_2Sb_2Te_5$ (left) and 80 nm $Ge_4Sb_1Te_5$ (right) with different heating rates leading to a change in the critical temperature T_C.

From the analysis of the variation of T_C with the heating rate an activation energy of 2.24 ± 0.11 eV is observed for $Ge_2Sb_2Te_5$ [6] and 3.72 eV ± 0.07 eV for $Ge_4Sb_1Te_5$, respectively.

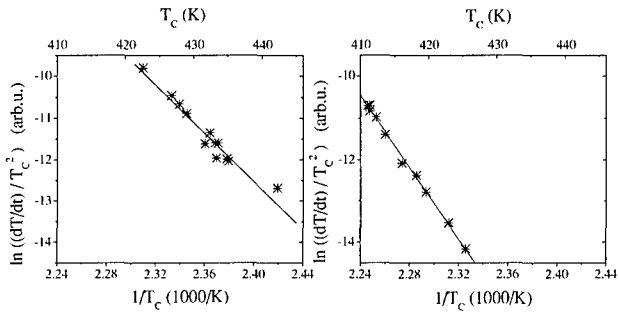

Figure 2. The activation energy E_A of the amorphous to crystalline transition at T_C is determined from Kissinger plots: (left) The slope of the linear fit determines the activation energy to 2.24 ± 0.11 eV for $Ge_2Sb_2Te_5$ films [6].

The activation energy for the $Ge_4Sb_1Te_5$ films is determined to 3.72 eV ± 0.07 eV. To determine the nature of the transformation XRD scans of 200 nm thin $Ge_2Sb_2Te_5$ and $Ge_4Sb_1Te_5$ films were performed after different isothermal annealing steps (figure 3). After deposition the films are amorphous. Crystallization into the rock salt cubic phase is observed at 415 K for $Ge_2Sb_2Te_5$ and at 430 K for $Ge_4Sb_1Te_5$. For $Ge_2Sb_2Te_5$ a second phase is formed after annealing at 573 K. These peaks are characteristic for the formation of an hexagonal structure. This second phase transition for $Ge_2Sb_2Te_5$ has an activation energy of 3.64 ± 0.19 eV [6]. For $Ge_4Sb_1Te_5$ no hexagonal phase could be found for the annealing temperatures accessible.

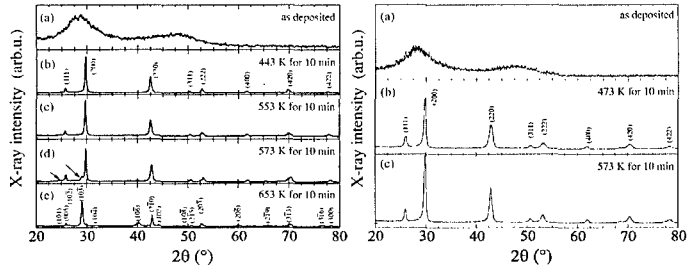

Figure 3. X-ray diffraction scans of 200 nm thin $Ge_2Sb_2Te_5$ (left) and $Ge_4Sb_1Te_5$ (right) films on Si substrates after different annealing procedures. Both annealing temperature and time are denoted. Left: diffraction pattern of (a) an amorphous $Ge_2Sb_2Te_5$ film, (b)-(d) rock salt structure and (e) hexagonal structure. The arrows in (d) indicate the changes due to beginning transition from the rock salt to the hexagonal structure. Right: diffraction pattern of (a) an amorphous $Ge_4Sb_1Te_5$ film, (b) and (c) of rock salt structure. For $Ge_4Sb_1Te_5$ no hexagonal structure could be found.

Interesting insight into the crystallization mechanism is obtained by plotting the activation energies for crystallization of several compounds along the pseudo-binary line against the number of Ge-Te bonds. In figure 4 data obtained from our measurements as well as literature data [2] are shown. It is noteworthy that there is a clear correlation between the activation energy for crystallization and the amount of Ge-Te bonds. This indicates that the kinetics of crystallization are controlled by the energetics of the Ge-Te bond. In addition, this result is in good agreement with several structural studies which show a very strong preference for Ge and

Te atoms to occupy different lattice sites, i.e. A and B sites in the rock salt lattice [2,9]. This is evidence for a strong Ge-Te bond, which is apparently also related to the activation energy for crystallization. Hence, this activation energy can be varied just by varying the amount of Ge-Te-bonds.

Even though this figure already suggests how activation energies for crystallization can be tailored through the film stoichiometry, it does not yet provide any detailed understanding of the microscopic mechanism of crystallization.

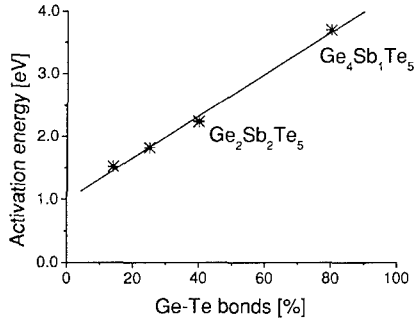

Figure 4. A summary of activation energies of several phase change materials as function of Ge-Te bonds in the material. The values are obtained from our electrical resistance measurements and literature data [2]. There is a strong correlation between activation energy and the number of Ge-Te bonds in the phase change material.

For a microscopic understanding power-time-effect diagrams for amorphous 85 nm films $Ge_2Sb_2Te_5$ and $Ge_4Sb_1Te_5$ were recorded with the static tester. These diagrams, displayed in figure 5, show the reflectance change at 830 nm upon variable laser irradiation.

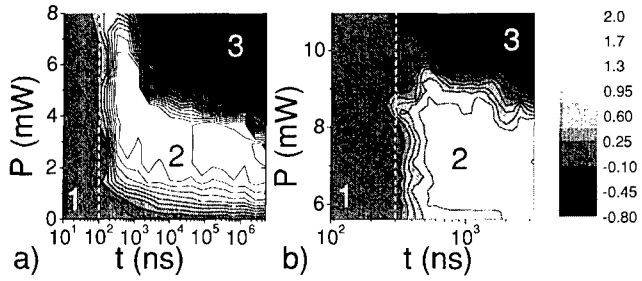

Figure 5. Power time effect diagrams of a) 85 nm thin amorphous of $Ge_2Sb_2Te_5$ films on glass and b) 85 nm thin amorphous films of $Ge_4Sb_1Te_5$ on glass. The diagrams show the relative reflectance change (%) upon absorbed power P (mW) as function of the pulse duration t (ns). A reflectance increase is assigned to crystallization, a decrease of reflectance to ablation. A missing reflectance change shows that no crystallization has taken place. A minimum time of 100 ns for $Ge_2Sb_2Te_5$ and 300 ns for $Ge_4Sb_1Te_5$, respectively, is needed to crystallize the materials.

Both diagrams show 3 regions. In region 1 the reflectance change is zero and thus the pulse is to weak to crystallize. In region 2, the material crystallizes and in region 3 the pulse is strong enough to ablate the irradiated area. Furthermore, both materials need a minimum time until crystallization starts. For $Ge_2Sb_2Te_5$ a minimum time of 100 ns is needed and for $Ge_4Sb_1Te_5$ 300 ns are required, respectively.

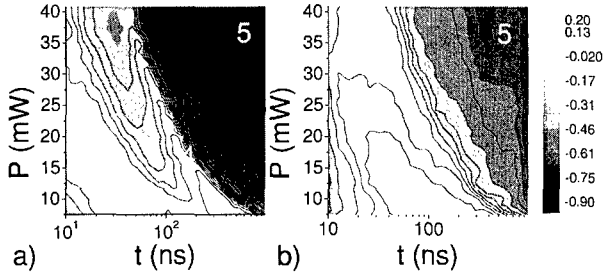

Figure 6. Power-Time-Effect diagram of a) 80 nm cubic crystalline $Ge_2Sb_2Te_5$ on glass and b) 80 nm cubic crystalline $Ge_4Sb_1Te_5$ on glass. The diagrams show the relative reflectance change (%) upon absorbed power *P* (mW) as function of the pulse duration *t* (ns) after a an amorphous bit has been written. A reflectance increase is assigned to recrystallization, a decrease of reflectance to amorphization. In region 1 no recrystallization takes place. In region 2 recrystallization takes place and in region 3 amorphization is observed. In region 4, which only occurs for the $Ge_2Sb_2Te_5$ material melt crystallization occurs and finally in region 5 the film ablates.

Since recrystallization is the more important transformation power-time-effect diagrams were recorded for 80 nm thick crystalline films of $Ge_2Sb_2Te_5$ and $Ge_4Sb_1Te_5$ with NaCl structure. The corresponding diagrams are shown in figure 6. Again, several regions can be distinguished. In region 1 the pulses are to weak to recrystallize while in region 2 recrystallization takes place. In region 3 the pulse melts the material but due to the short pulse duration the material can not relax into the crystalline state and remains amorphous. Then $Ge_2Sb_2Te_5$ shows melt crystallization in region 4. In region 5 the irradiated material is ablated. The minimum pulse durations needed for recrystallization is below 10 ns for $Ge_2Sb_2Te_5$ and about 16 ns for $Ge_4Sb_1Te_5$. Thus, recrystallization proceeds much faster than crystallization and the material with the lower macroscopic activation barrier also recrystallizes faster. We have shown that $Ge_2Sb_2Te_5$, in agreement with previous data [9,10], recrystallizes by the growth of sub critical nuclei, while $Ge_4Sb_1Te_5$ grows from the bit rim [11].

The fact that recrystallization can proceed by two different mechanisms opens different strategies to boost performance. For growth dominated recrystallization increasing the temperature upon recrystallization is a straight forward approach to enhance diffusion. For nucleation dominated growth on the contrary the influence of surrounding dielectric layers could be exploited.

To obtain a larger database to extract similar correlations combinatorial concepts can be applied. Hence a Sb_xTe_{1-x} sample has been prepared for which x varies over the sample. The areas investigated with the static tester had the compositions of $Sb_{25}Te_{75}$, $Sb_{29}Te_{71}$ and $Sb_{32}Te_{68}$. The power-time-effect diagrams are shown in figure 7.

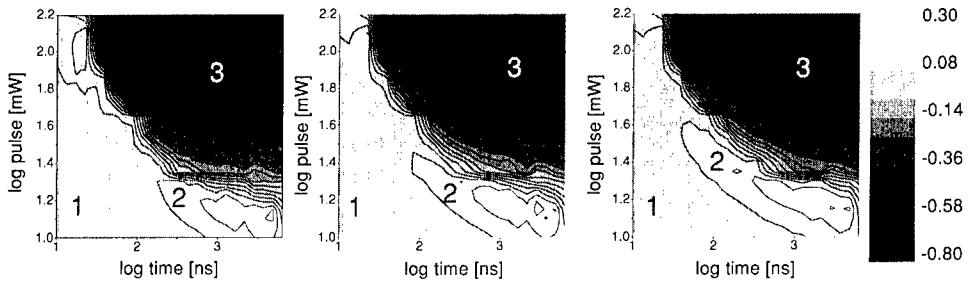

Figure 7. Power time effect diagrams of 60 nm of amorphous Sb_xTe_{1-x} on glass. The diagrams show the relative reflectance change (%) upon absorbed power P (mW) as function of pulse duration t (ns). The stoichiometries measured with SNMS are changing from $Sb_{27}Te_{75}$, to $Sb_{29}Te_{71}$ and $Sb_{32}Te_{68}$. Region 2 shifts to shorter minimum crystallization times with decreasing Sb amount.

The shift of region 2 to the left means that the minimum times needed for crystallization decreases with Sb amount. This, still somewhat preliminary result already indicates that the use of combinatorial concepts will enable a faster determination of crucial factors which control the kinetics. Hence this can be exploited to push the materials to the achievable limits needed for ultra fast phase change recording.

ACKNOWLEDGEMENTS

The authors like to thank J. Larscheid for technical support. Financial support by the Fonds der Chemischen Industrie is gratefully acknowledged.

REFERENCES

1. J. Gonzales-Hernadez, B.S. Chao, D. Strand, S.R. Ovshinsky, D. Pawlik and P. Gasiorowski, Appl. Phys. Commun. **11** (1992) 557
2. N. Yamada, MRS Bulletin **21** (9),48-50 (1996)
3. V. Weidenhof et al., J. Appl. Phys. **86** (10), 5879 (1999)
4. V. Weidenhof et al., J. Appl. Phys. **88** (2), 657 (2000)
5. L.J. van der Pauw, Philips Res. Rep. **13**, 1 (1958)
6. I. Friedrich et al., J. Appl. Phys. **87** (9), 4130 (2000)
7. R. Glang, in *Handbook of Thin Film Technology*, edited by L.I. Maissel and R. Glang (McGraw-Hill Book company, New York) chap. 1
8. H. E. Kissinger, Anal. Chem. **29**, 1702 (1959)
9. J. H. Coombs et al. J. Appl. Phys. **78** (1995), 4918
10. J. Park et al., Jpn. J. Appl. Phys. **38** (1999) 4775
11. St. Ziegler et al., (private communication).